Reconciling real hysteresis with the Masing conditions via Masing manifolds

J. H. Porter, M. R. W. Brake, M. M. Karpov
William Marsh Rice University, Department of Mechanical Engineering,
6100 Main St., Houston, TX 77005, USA
e-mail: **brake@rice.edu**

Abstract
The Masing conditions establish a criterion to relate the loading curve of a hysteretic system to its complete hysteresis loop. For the field of joint mechanics, where the hysteresis describes the dissipative, tangential behavior within an interface, the Masing conditions allows for significant computational savings. In practice, though, jointed systems experience time varying normal forces that can modify the tangential behavior of the system. Consequently, the hysteretic behavior of the system does not adhere to the Masing conditions. In this work, this discrepancy between the Masing conditions and behavior exhibited by real systems is explored. Specifically, an additional condition is introduced that results in a manifold, which spans the tangential displacement-tangential force-normal force space. Several prototypical systems are investigated, and the preliminary results show that the hysteresis of these systems conforms to the three dimensional manifold even though it does not conform with the original Masing conditions.

1 The Masing conditions

The Masing conditions [1, 2, 3, 4] stipulate that, for steady state responses, the hysteretic behavior of a system can be uniquely determined from the loading curve formed by taking a system at rest and loading it to its maximum steady state displacement. This loading curve is related to the steady state hysteresis loop via

1. The forward portion of the hysteresis loop is identical to the initial loading curve except that it is scaled by a factor of two such that it begins at the smallest displacement and extends to the largest displacement (which is typically from $-u_{max}$ to $+u_{max}$).
2. The reverse portion of the hysteresis loop is identical to the forward portion, only rotated 180° with respect to the center of the hysteresis loop.
3. The hysteretic response is determined from the last point of the loading cycle before a reversal; if the loading curve crosses a previous loading curve, then it must conform to the previous loading curve.

These conditions are illustrated in Fig. 1.

The use of the Masing conditions greatly simplifies the calculation of hysteretic behavior as only the initial loading curve needs to be calculated in order to deduce the entire hysteresis loop. In particular, this is the fundamental concept behind the use of quasi-static modal analysis [6, 7] for calculating the hysterestic behavior of a jointed system. If the Masing conditions cannot be used, then it can be five times more expensive to calculate the hysteretic behavior of a system [5, 8] as the initial loading curve, first unloading curve, and first reloading curve all need to be calculated. This is the difference between only calculating the curve shown in step one of Fig. 1 and calculating all of the curves shown in steps one, two, and three of Fig. 1.

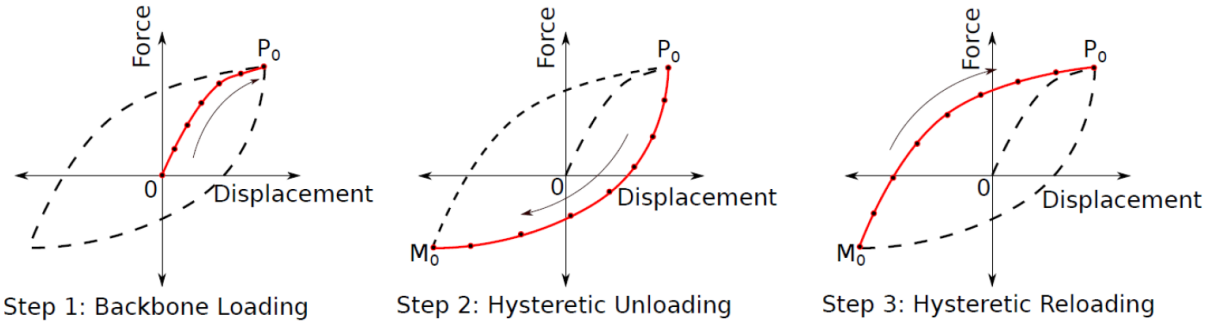

Figure 1: Illustration of the Masing conditions. The curves in steps two and three are scaled (and rotated) versions of the curve in step one. Modified from [5].

2 Breakdown of the Masing conditions

In real jointed structures, the normal force across an interface is known to vary during excitation [9, 10]. As a result, the tangential friction force, which is often conceptualized as being related to the normal force by a scalar (i.e., Coulomb's friction coefficient, μ), is modulated during excitation. This can result in non-symmetric hysteresis loops that violate Masing's conditions, as shown in Fig. 2[1].

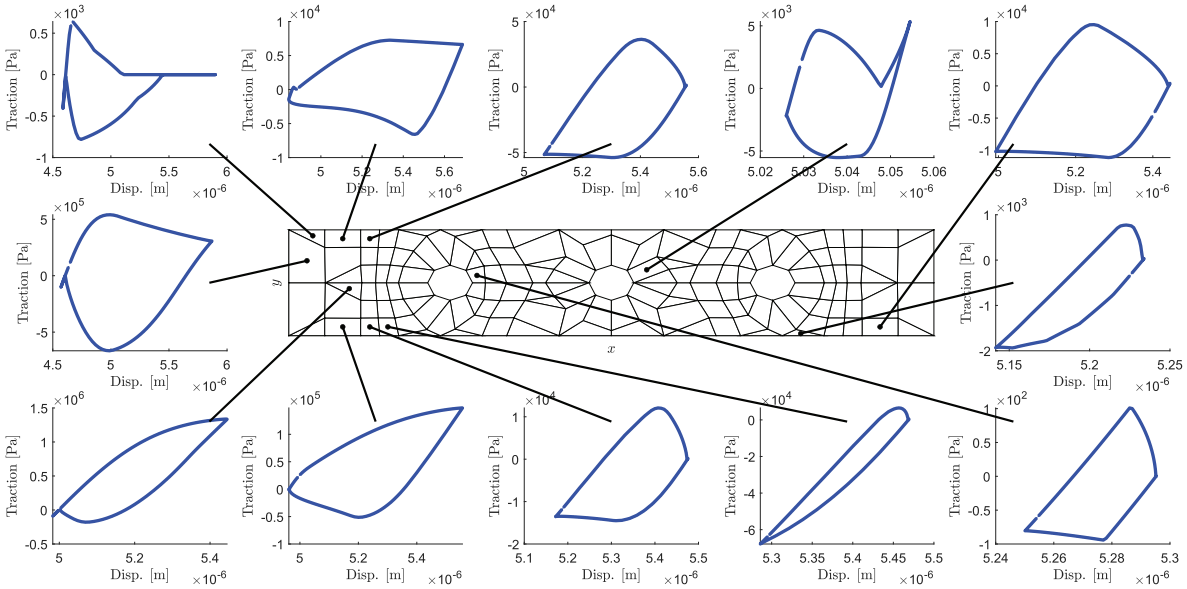

Figure 2: Hysteresis loops from a tribomechadynamics model of a jointed interface in which the normal load is allowed to vary throughout the simulation due to the external excitation. Modified from [11].

At the elemental level, the hysteretic model for the loops shown in Fig. 2 could be described as elastic dry friction. Similar to a Jenkins element, elastic dry friction is defined for the *initial* loading curve[2] as

$$f = \begin{cases} k_T u(t) & k_T u(t) < \mu N(t) \\ \mu N(t) & \text{Otherwise} \end{cases} \tag{1}$$

[1] For details of how these hysteresis loops were calculated, the reader is referred to [11, 8].

[2] For simplicity, the equations are only provided for loading from rest until a maximum displacement.

in terms of the tangential stiffness k_T, displacement u, time t, and normal force N. As $\mu N(t)$ is non-constant, this results in a hysteresis loop that can collapse (i.e., go to zero as the interface separates), have sudden spikes (e.g., when a pressure wave propagates across the interface), or even exhibit a slip force that decreases with time for one portion of the loading curve but not the other (e.g., the bottom left hysteresis loops in Fig. 2). These observations lead to the hypothesis:

> **Hypothesis:** If the Masing conditions accounted for time varying normal force then they would be more broadly applicable to real jointed structures.

If this hypothesis is supported, then the modified Masing conditions would result in a response manifold that governed the hysteretic, steady-state behavior of a system. A two-dimensional section of this manifold for a constant normal force would result in the original Masing conditions. However, once the normal force begins to vary, the tangential force-displacement response must be extended into the third dimension, normal force.

3 Criteria to remain on manifold

3.1 Normal load decreasing in stuck section

Upon load reversal, the equation of the manifold is

$$f_{manifold} = k_t(u(t) - u_0) + sign(f_0)\mu N(t) \tag{2}$$

This must be equal to the equation of the current force which is evaluated as

$$f_{eldry} = k_t(u(t) - u_0) + sign(f_0)\mu N_0. \tag{3}$$

This will only be satisfied if $\mu N_0 = \mu N$. This leads to frequent deviations from the manifold in the model. The force f_{eldry} is consistent with an anchor and spring representation of the friction model (with varying normal load), so it is not clear what the physical interpretation of using the $f_{manifold}$ would be.

Alternatively, the manifold may be modified such that the hysteresis loop remains on the manifold. This would consist of oscillating between equal anchor displacements (i.e., points where the tangential force is zero). This means that equality is achieved in the above equations by varying u_0 as a function of N. For the single slider representation, this would result in larger oscillation amplitudes at higher normal loads. However, such a model does not necessarily make physical sense where amplitudes of vibration would be expected to be higher for less normal and thus less tangential force resisting vibration. Furthermore, such a modification to the manifold is not possible for two or more elements in parallel since they would generally require different displacement amplitudes. Oscillating between equal anchor displacements also requires the condition that

$$\frac{d}{du_t}[\mu N] \geq -k_t \quad \forall f_{eldry} \text{sign}(u(t) - u_0) < 0 \tag{4}$$

This prevents the anchor from slipping in the opposite direction of motion due to a rapid drop in normal force immediately after reversal.

3.2 Normal load increasing in slipped section

The update for elastic dry friction indicates that the fastest rate of increase possible in tangential force is k_t. To remain on the manifold, once the system has started slipping it must remain slipping until the next reversal point. This requires that the tangential force always increase as fast as μN. This results in the condition that

$$\frac{df}{d\tau} = \frac{d}{d\tau}[\mu N] \tag{5}$$

for a dummy variable τ used to parameterize the displacement and load histories. This can be converted to

$$\frac{d}{du_t}\left[\mu N\right] = \frac{df}{du_t} \leq k_t. \tag{6}$$

While this condition can be satisfied for a range of harmonic amplitudes of N, the condition must hold for all times that the system is slipping. Therefore, phase differences between N and u_t can easily result in violations of this condition.

4 Preliminary simulations

To test the hypothesis, a series of numerical experiments are proposed. In this extended abstract, the first of these, a single degree of freedom oscillator with a time varying normal force, is considered. The friction behavior of the oscillator is described by the elastic dry friction element (Eq. 1). Assuming arbitrary parameters ($\mu = 0.1$, $u_{max} = 1$, $k_T = 1$, and tangential displacement frequency $\omega = 2\pi$), the Masing manifolds are able to be calculated for a number of different normal force functions. As shown in Fig. 3, these include a constant normal force ($N = 5$, Fig. 3(a)-(b)), and sinusoidally varying normal forces of $N = \sin(\omega t) + 5$ (Fig. 3(c)-(d)), $N = \sin(2\omega t) + 5$ (Fig. 3(e)-(f)), and $N = \max(0, 4\sin(2\omega t) + 3)$ (Fig. 3(g)-(h)).

In order for the hysteresis loops to remain on the Masing manifold, there is one caveat: the force at reversal that the subsequent loading cycle is based upon must scale with the time varying normal force. That is, upon a load reversal that occurs at a displacement u_0 with force f_0, the subsequent loading cycle is governed by

$$f = \begin{cases} k_T(u(t) - u_0) + \text{sign}(f_0)\mu N(t) & |k_T(u(t) - u_0) + \text{sign}(f_0)\mu N(t)| < \mu N(t) \\ \mu N(t)\text{sign}(u(t) - u_0) & \text{Otherwise} \end{cases} \tag{7}$$

for a system that is slipping. Without this condition, the hysteresis loop deviates from the Masing manifold during the stuck phase of the loading cycle. For this particular hysteresis model, the stuck regime is independent of the normal force. Thus, no further scaling is needed for a system that never slips. For a more general hysteresis model, in which the tangential stiffness/stuck regime depends upon the normal force, a relationship similar to Eq. 7 can be derived.

The hysteresis loops shown in Fig. 3(a), (c), (e), and (g) each fall upon the corresponding Masing manifolds. In some cases, such as for $N = \sin(\omega t) + 5$ (Fig. 3(c)-(d)), the hysteresis loop is not symmetric. As the form for $N(t)$ becomes more complicated, the deviation of the hysteresis loops from the one formed by the traditional Masing conditions (i.e., $N = 5$, Fig. 3(a)-(b)) increases; however, each of the four hysteresis loops still conform to the Masing manifold.

5 The revised Masing conditions

Based on the preliminary work shown here, in which the fundamental hypothesis relating the Masing conditions to the normal force cannot be rejected, a revision to the Masing conditions, collectively referred to as the Masing manifold, is proposed. For the steady-state oscillation of a system between two extremum, the resulting hysteretic behavior is described by the manifold in the tangential displacement-tangential force-normal force space constructed according to:

1. In order to consider constructing a Masing manifold, it is paramount that the hysteretic behavior for a constant normal force conforms to the Masing conditions (this implies that Bouc-Wen models will not be generally admissible).

2. The initial loading curve is defined as the tangential force-tangential displacement relationship, parameterized in terms of the normal force, calculated from rest to the maximum displacement.

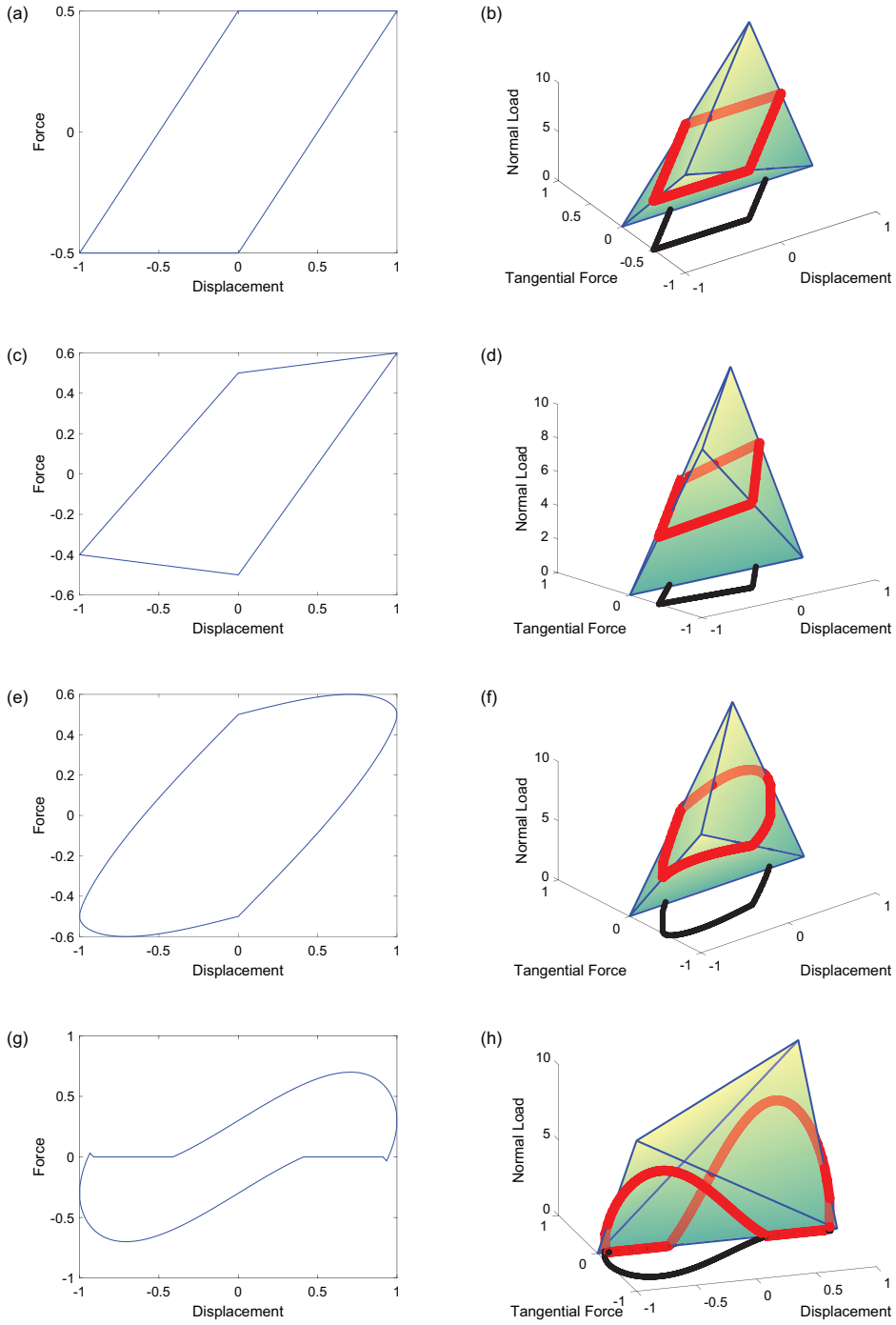

Figure 3: Hysteresis loops and Masing manifolds for (a) and (b) constant normal force, (c) and (d) sinusoidally varying in phase normal force, (e) and (f) sinusoidally varying normal force at twice the frequency of the tangential displacement, (g) and (h) sinusoidally varying normal force that goes to zero. All results are from the elastic dry friction model. The black curves on the right plots are the projections of the hysteresis loops onto the $N = 0$ plane for visualization purposes.

3. The forward loading curve of the hysteresis loop is the initial loading curve scaled by a factor of two (to account for oscillating between $-u_{max}$ and u_{max}) and terminating at the same location as the initial loading curve.

4. The backward loading curve of the hysteresis loop is identical to the forward loading curve rotated

180° about the origin, beginning at the end of the forward loading curve and ending at the start of the forward loading curve.

5. As the normal force changes, the reference force from the last load reversal must scale with the normal force.

While this preliminary work has demonstrated the concept of a Masing manifold for the simple, elastic dry friction hysteresis model, it still must be generalized to other friction models. Thus, future work must seek to assess the validity of the Masing manifold for studying both more complex hysteresis models (such as Bouc-Wen and Iwan models), and more complex system models (e.g., [12]).

References

[1] G. Masing, "Self-stretching and hardening for brass," *Proceedings of the Second International Congress for Applied Mechanics*, pp. 332–335, 1926.

[2] D. J. Segalman, "A four-parameter Iwan model for lap-type joints," *ASME Journal of Applied Mechanics*, vol. 72, pp. 752–760, 2005.

[3] M. R. W. Brake, Ed., *The Mechanics of Jointed Structures*. Springer, 2017.

[4] A. T. Mathis, N. N. Balaji, R. J. Kuether, A. R. Brink, M. R. W. Brake, and D. D. Quinn, "A review of damping models for structures with mechanical joints," *Applied Mechanics Reviews*, vol. 72, p. 040802, 2020.

[5] N. N. Balaji and M. R. W. Brake, "An efficient quasi-static non-linear modal analysis procedure generalizing Rayleigh quotient stationarity for non-conservative dynamical systems," *Computers and Structures*, vol. 230, pp. 106 184 (1–16), 2020.

[6] M. S. Allen, R. M. Lacayo, and M. R. W. Brake, "Quasi-static modal analysis based on implicit condensation for structures with nonlinear joints," in *International Conference on Noise and Vibration Engineering*, Leuven, Belgium, September 2016.

[7] R. M. Lacayo and M. S. Allen, "Updating structural models containing nonlinear Iwan joints using quasi-static modal analysis," *Mechanical Systems and Signal Processing*, vol. 114, pp. 413–438, 2019.

[8] J. H. Porter, N. N. Balaji, C. R. Little, and M. R. W. Brake, "A quantitative assessment of the model form error of friction models across different interface representations for jointed structures," *Mechanical Systems and Signal Processing*, vol. 163, p. 108163, 2022.

[9] T. Dreher, M. R. W. Brake, B. Seeger, and M. Krack, "In situ, real-time measurements of contact pressure internal to jointed interfaces during dynamic excitation of an assembled structure," *Mechanical Systems and Signal Processing*, vol. 160, p. 107859, 2021.

[10] A. R. Brink, R. J. Kuether, M. D. Fronk, B. L. Witt, and B. L. Nation, "Contact stress and lienarized modal predictions of as-built preloaded assembly," *ASME Journal of Vibration and Acoustics*, vol. 142, p. 051106, 2020.

[11] J. H. Porter, N. N. Balaji, and M. R. W. Brake, "A non-masing microslip rough contact modeling framework for spatially and cyclically varying normal pressure," in *39th International Modal Analysis Conference (IMAC XXXIX)*, Online, February 2021.

[12] N. N. Balaji, W. Chen, and M. R. W. Brake, "Traction-based multi-scale nonlinear dynamic modeling of bolted joints: Formulation, application, and trends in micro-scale interface evolution," *Mechanical Systems and Signal Processing*, vol. 139, pp. 106 615 (1–32), 2020.